Feasibility Study for 3D Imaging of Hot Spot in Activated Concrete Wall Using Large-Area Compton Camera (LACC)

Jae Hyeon Kim [a], Young-su Kim [a], Junyoung Lee [a], Chan Hyeong Kim [a*]
[a]*Dept. Of Nuclear Engr., Hanyang Univ., 222 Wangsimni-ro, Seongdong-gu, Seoul 04763, Korea*
[*]*Corresponding author: chkim@hanyang.ac.kr*

1. Introduction

When decommissioning large facilities such as cyclotrons or nuclear power plants, it is essential to reduce the disposal costs of radioactive waste. For this, the massive materials such as a concrete shielding wall should be classified in terms of their activity levels.

However, the neutron-induced activation of a metal subject in concrete can result in hot-spot contamination which may classify the concrete wall as long-lived low and intermediate level waste (LILW-LL). The hot-spot contamination will increase average activity of the concrete wall. By imaging and removing the hot-spot contaminations, the low-activated concrete part can be regarded as exempt waste (EW), resulting the reduction of disposal costs.

For the application of the radioactive contamination monitoring, we developed a high-performance Compton imaging device, named Large-Area Compton Camera (LACC) [1]. In the present study, Monte Carlo simulation was performed to investigate the feasibility of the LACC for imaging of the hot-spot in the neutron-induced activated concrete wall. First, by using MCNP and FISPACT codes, the neutron-induced radioactivities of the concrete wall and the rebar were calculated, and the activated environment of the concrete wall was modeled. Then, by using Geant4, we estimated the feasibility of the LACC for imaging hot-spots with different activities in the activated reinforced concrete wall.

2. Neutron-Induced Activation Calculation

In the present study, to calculate neutron-induced activation, we considered a shielding reinforced concrete wall for cyclotron facility. The cyclotron was assumed to have operated to produce ^{18}F by the nuclear reaction with 18 MeV proton and $H_2{}^{18}O$ (95% enriched) target for 11 years. Then, this study calculated the activities of the radioisotopes produced from the concrete and rebar after the cooling time of 2.25 years. MCNP6.1.1beta [2] and FISPACT-2010 [3] codes were used to calculate the neutron-induced radioactivities of the activated concrete wall and rebars. A reinforced concrete wall containing five rebars was modeled in MCNP (Fig. 1). The dimension of the concrete wall was 1 m × 1 m × 1 m, and the rebar had a diameter of 5 cm. The target was placed at 0.5 m distant from the concrete wall. The concrete wall was composed of ordinary concrete [4]. Because the infinitesimal concentrations of Co, Cs, and Eu are normally present in concrete and become long-lived activated products such as ^{60}Co, ^{134}Cs, and ^{152}Eu, this study also considered the concentrations in the concrete. The concentrations of Co, Cs, and Eu were assumed to have the weight fractions of 9.54×10^{-4}%, 1.11×10^{-4}%, and 8.58×10^{-5}%, respectively [5]. The rebars in the reinforced concrete wall were made up of steel, assuming that the concentration of Co exists with the weight fraction of 0.38% [6].

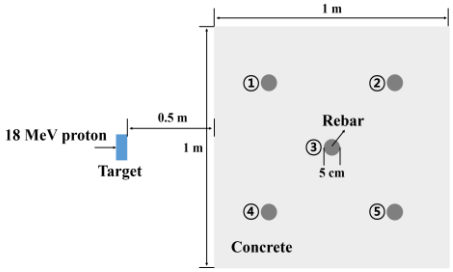

Fig. 1. Configuration of target and the reinforced concrete wall in MCNP and FISPACT.

The neutron energy distribution, obtained by the nuclear reaction with 18 MeV proton and the target, was used as the neutron source. Then, the neutron fluences in the concrete wall and rebar were calculated by F4 tally in MCNP. For the simulation, ENDF71x was used as the neutron cross-section data in MCNP, and VITAMIN-J, which was provided in the EAF-2010 library, was used as the decay data in FISPACT code, respectively.

After the cooling time of 2.25 years, the results showed that ^{55}Fe, ^{152}Eu and ^{60}Co were mainly produced from the activated concrete wall. Because ^{55}Fe is a beta-emitting isotope, this study only considered ^{152}Eu and ^{60}Co which are gamma-emitting isotopes. The specific activities of ^{152}Eu and ^{60}Co were calculated to be 2.15×10^3 Bq/kg and 6.59×10^2 Bq/kg. For the rebars, after the cooling time, the main products by the neutron activation were also ^{55}Fe and ^{60}Co. The specific activities of ^{60}Co were calculated to be 6.38×10^5 Bq/kg, 2.47×10^4 Bq/kg, 1.80×10^5 Bq/kg, 5.89×10^5 Bq/kg, and 2.33×10^4 Bq/kg for rebar 1 to rebar 5, respectively. The results showed that ^{60}Co was produced in the most activated rebar nearly a thousand times more than in the concrete. From these results, the rebar will be regarded as high-activation part in the activated concrete.

To model the activated concrete wall, the ^{152}Eu and ^{60}Co were assumed to be distributed in the concrete wall

uniformly. The rebars were assumed to contain ^{60}Co uniformly with their specific activities. The hot spots with different activities (1 μCi, 5 μCi, and 10 μCi.) were assumed to be placed in the concreate wall which is made of concrete and rebars.

3. Feasibility Study for Internal Imaging in Neutron-Induced Activated Concrete Wall

Geant4 (version 10.04.p02) [7] was used to model the LACC, and to demonstrate the imaging capability of the LACC for the hot-spot in the neutron-induced activated concrete wall. For the simulation, the structure of the LACC was modeled in detail in Geant4. The LACC consisted of two monolithic NaI(Tl) scintillation detectors coupled to an array of 36 square-type PMTs. The NaI(Tl) scintillators had an area of 27 cm × 27 cm, and the thicknesses were 2 cm for the scatter detector and 3 cm for the absorber detector, respectively. The distance between the scatter and the absorber detector was 25 cm. For the realistic simulation, we applied the energy resolution and spatial resolution which were evaluated from the previous study [8]. G4EmLivermorePhysics was used for the physics library in Geant4.

A reinforced concrete wall with a size of 1.0 m × 1.0 m × 1.0 m, which was considered in Section 2, was modeled to be placed at the surface of the LACC. The concrete wall was assumed to contain ^{152}Eu and ^{60}Co uniformly, of which the gamma energies are 0.96 MeV, 1.08 MeV, 1.11 MeV, and 1.41 MeV for ^{152}Eu and 1.17 MeV and 1.33 MeV for ^{60}Co. For the gamma-rays from ^{152}Eu, we only considered the gamma-rays whose branching ratios are larger than 0.1.

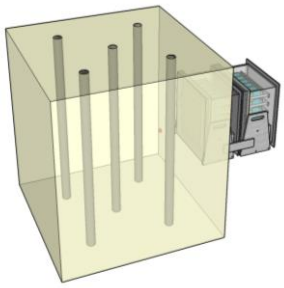

Fig. 2. Configuration of an activated reinforced concrete wall containing a hot-spot contamination and large-area Compton camera.

To demonstrate the imaging capability for a hot-spot contamination in the activated reinforced concrete wall by the LACC, a simulation was performed in Geant4. The simulation was carried out with the activated concrete wall containing the activated rebars, in which a ^{60}Co hot spot is placed. Five rebars with a diameter of 5 cm were located at the center positions of (±25 cm, 0, 25 cm), (0, 0, 50 cm), and (±25 cm, 0, 75 cm), respectively, when the position of (0, 0, 0) was the center position of the front surface of the LACC.

As a hot-spot contamination, a ^{60}Co point-source was also modeled to be placed in the activated concrete wall including the activated rebars. Fig. 2 shows the configuration of the simulation. In the simulation, the coordinate of the ^{60}Co hot-spot was (–10 cm, 0, 25 cm) in the concrete wall. We performed the simulations by changing the activity of the source as 0 μCi (no hot-spot), 1 μCi, 5 μCi, and 10 μCi. Considering a three-minute measurement, the numbers of emitted gamma-rays from the 1 μCi ^{60}Co point-source were 6.66×10^6 for 1.17 MeV and 1.33 MeV, respectively. For the concrete wall, 2.76×10^8 gamma-rays of 1.17 MeV and 1.33 MeV from ^{60}Co, and total 5.31×10^8 gamma-rays from ^{152}Eu were emitted from the wall uniformly. For the rebars, 4.06×10^9 gamma-rays of 1.17 MeV and 1.33 MeV were emitted from all rebars (i.e., 1.78×10^9, 6.9×10^7, 5.03×10^8, 1.64×10^9, and 6.5×10^7 gamma-rays from rebar 1 to rebar 5, respectively).

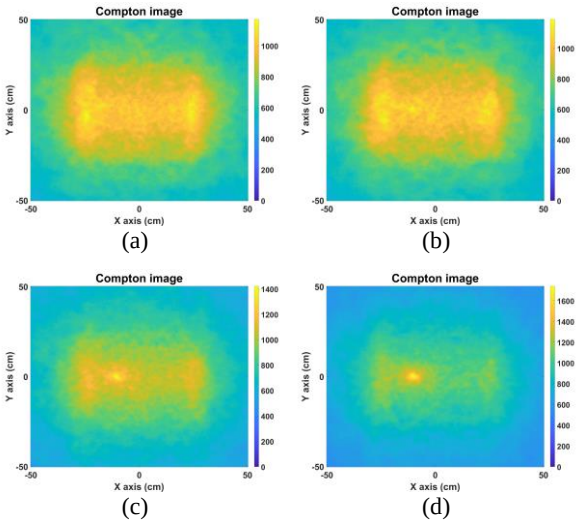

Fig. 3. Reconstructed Compton images for no hot-spot (a), and ^{60}Co hot-spot of 1 μCi (b), 5 μCi (c), and 10 μCi (d) in an activated reinforced concrete wall.

We obtained the Compton images for the hot-spot using simple back projection (SBP) algorithm. The energy window from 1.1 MeV to 1.4 MeV was applied to reconstruct the Compton image. The reconstructed Compton images for the simulation were shown in Fig. 3. In the reconstructed images, the approximate structure of the rebar was well represented without any hot-spots in the activated concrete wall (Fig. 3(a)). For the hot-spot of 1 μCi, the locations of the hot-spot were strugglingly seen comparing with the image without hot-spots (Fig. 3(b)). For the hot-spot of 5 μCi and 10 μCi, the Compton images show the locations of the hot-spot clearly, and the locations of the hot-spot were localized accurately at the true position (Fig. 3(c) and Fig. 3(d)). These results show that the LACC can be used to image

the hot-spot and the internal structure in the activated concrete wall.

4. Conclusions

In the present study, the feasibility of the LACC for imaging the hot-spot contamination in the activated reinforced concrete wall was studied. To modeled the activated concrete wall, the activation calculation was performed by MCNP and FISPACT code. The activation calculation results show that ^{55}Fe, ^{152}Eu, and ^{60}Co were main products, and ^{60}Co was produced in the rebar a thousand times more than in the concrete. Then, Geant4 was used to confirm the imaging capability of the LACC for hot-spot in the activated concrete wall containing the activated rebar. The results show that the LACC can image the hot-spot in the activated concrete wall. The results of this study contributed to demonstrate the potential of the LACC for the application of the radioactive contamination monitoring, especially hot-spot in a concrete wall. It can be concluded that the LACC can be used to reduce the disposal costs and enhance the safety for the decommissioning.

REFERENCES

[1] Y.-S. Kim *et al*., Development and performance evaluation of large-area Compton camera, *Transactions of the Korean Nuclear Society Spring meeting*, May 17–19, Jeju, 2017.
[2] T. Goorley *et al.*, Initial MCNP6 Release Overview, *Nucl. Technol.*, vol. 180, no. 3, pp. 298–315, 2012.
[3] R. A. Forrest, FISPACT-2007: User manual, *UKAEA FUS-534 report*, 2007.
[4] National Council on Radiation Protection and Measurements (NCRP), Radiation Protection for Particle Accelerators Facilities, *NCRP Report No. 143*, 2011.
[5] S. Alhajali *et al.*, Estimation of the activation of local reactor shielding concretes, *Prog. Nucl. Ener.*, Vol. 51, No. 2, pp. 374–377, 2009.
[6] A. S. Zhilkin *et al.*, Cobalt and other impurities in reactor steels, *Atom. Ener.*, Vol. 52, No. 4, pp. 264–266, 1982.
[7] S. Agostinelli *et al.*, GEANT4 - A simulation toolkit, *Nucl. Instruments Methods Phys. Res. Sect. A Accel. Spectrometers, Detect. Assoc. Equip.*, vol. 506, no. 3, pp. 250–303, 2003.
[8] Y.-S. Kim *et al.*, Position-sensitive NaI(TL) detector module for large-area Compton camera, *J. Korean Phys. Soc.*, vol. 72, no. 1, 2018.